EMAT GENERATION AND LASER DETECTION OF SINGLE LAMB WAVE MODES

Zhiqi Guo, J. D. Achenbach, and Sridhar Krishnaswamy

Center for Quality Engineering and Failure Prevention
Northwestern University
Evanston, IL 60208

INTRODUCTION

Non-contact and couplant-free nondestructive testing methods are desired in certain situations. There are several designs of non-contact transducers that have been developed. Electromagnetic acoustic transducers (EMATs) and laser-based ultrasonic sensors are well known non-contact transducers. EMATs are typically of limited bandwidth. EMATs and LBU both have lower sensitivity than conventional piezoelectric transducers, and are therefore typically useful in situations where there is sufficient signal strength, but where non-contact is necessary (EMATs and LBU), or where high spatial resolution (LBU) is needed. Thus, ultrasonic NDE schemes with various configurations have been utilized; these configurations include using EMATs as both generator and receiver [1-2], using lasers as both generator and receiver[3-4], and using a laser as source and EMATs as receiver [5].

In this work, testing of thin plates using Lamb waves is of interest. As is well recognized [6-7], Lamb waves are guided waves that can be used to interrogate the through-the-thickness structural integrity of plates over large distances, provided that complications associated with multiple modes and dispersion can be resolved. For practical applications, selecting an optimized single mode leads to higher sensitivity for detection of certain defect types. This implies that the mode and operation point in the frequency spectrum should be selectable. In this paper, EMAT generation of Lamb waves is employed. EMATs can provide a series of spatially periodic line sources on the surface of conductive objects. These line sources restrict the generated ultrasound to wave modes that are harmonically related to this spatial "forcing" wavelength, thus providing an attractive method to generate a single Lamb wave mode at a selectable operation point, as will be further discussed below.

To check whether indeed a single Lamb wave mode is generated, and to provide the high spatial resolution that is essential to monitor the scattering from small defects, a broadband path-stabilized Michelson laser interferometric detector is used to detect the scattered signal. This system has been successfully applied to an experimental investigation of the interaction of a single Lamb wave mode with a crack-like defect in a thin plate, which is described in detail in another paper [8]. Here we present results of an experimental detection of fatigue cracks in a riveted plate-structure.

EXPERIMENTAL SETUP

A schematic diagram of the EMAT-generation and laser-detection system is shown in Figure 1. The system includes the following devices:

- A tunable EMAT pulser/receiver unit which is used as the driver of an EMAT;
- A path-stabilized Michelson interferometer which is used as a detector;
- Related path stabilization feedback control circuits and a D/A plug-in board;
- Translation stage and controller;
- A digital oscilloscope as waveform monitor and A/D converter;
- A computer with graphical user interface programmed using Lab-Windows.

This is a computer controlled NDE system. The results are displayed on the computer screen after data processing.

Single Lamb Wave Mode Generation With a EMAT

The meander-line EMAT used in this work radiates energy through spatially periodic surface stresses. The generation of Rayleigh and Lamb waves by spatially periodic surface stresses has been investigated by Viktorov et al [9] and Thompson et al [10]. This spatially periodic line array source is used to excite Lamb waves in plates. The line spacing δ of the elements of the array acts as a "forcing" wavelength. Constructive and destructive interference takes place among the waves radiating from each line source, and only the wave modes of the same or harmonic "forcing" wavelength but of different frequencies will get excited. If the line array source is temporally driven by a narrow-band signal at the desired ultrasonic frequency, then only the particular Lamb wave mode with that frequency and harmonic "forcing" wavelength will get excited in the plate. The optimum spacing size of the EMAT's coil is $\delta=\lambda/2$ (half the wavelength of the selected wave mode).

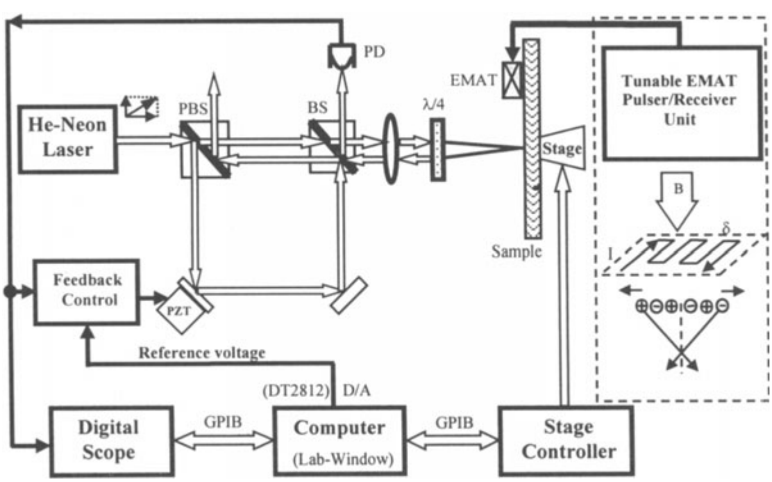

Figure 1. Schematic diagram of the EMAT generation and laser detection system.

The EMAT coil is driven by a tone-burst current at the desired ultrasonic frequency. The central frequency and number of cycles of the tone-burst may also be changed by the modulation control in order to obtain a different frequency bandwidth. There is an impedance matching circuit between the coil and the power driver to allow careful impedance matching adjustments. The specially designed EMAT is always operated at its electrically resonant state in order to obtain sufficient efficiency.

Broadband Detection by A Path-Stabilized Michelson Interferometer

In order to detect the Lamb waves generated by the EMAT, a broad-bandwidth and high-spatial resolution, path-stabilized Michelson interferometer was designed. The optical setup and the related path stabilization control circuits are shown schematically in Figure 1. The incident beam is split into two beams by a polarized beam splitter (PBS). The vertically polarized beam is reflected to the reference arm and the beam polarized horizontally is transmitted into the probing arm. In the probing arm, the beam first passes through a neutral beam splitter (BS), illuminates the surface of the sample and is reflected back. The horizontal polarization of the reflected probe beam is rotated by a quarter wave plate to the vertical polarized direction. In the reference arm, the beam is reflected by two mirrors, one of which is mounted on a PZT actuator for path stabilization purposes. The reference and the reflected probe beams, now both polarized vertically, are recombined by the BS to interfere with each other at the photo detector (PD).

The laser used here is a polarized Helium-Neon laser (5mW). Since the light intensity loss in the probing arm is much greater than that in the reference arm, the polarization plane of the laser is rotated to increase the component into the probing arm until the two beams have equal intensity at the detection plane. The output of the PD is proportional to the intensity I which is given by equation (1):

$$I = I_p + I_r + 2\sqrt{I_p I_r} \cdot \cos(4\pi \Delta d/\lambda) \tag{1}$$

where $\Delta d = \Delta d_{sc} + d_{ac}$.

Here λ is the wavelength of the laser being used, I_p and I_r are the light intensities of the probing arm and the reference arm, respectively, and Δd, Δd_{sc} and d_{ac} are total path difference, static path difference, and path difference due to the out-of-plane displacement, respectively.

Because the displacements associated with ultrasonic wave propagation are small compared to the wavelength of the laser, only local oscillations about a point on the response function Equation (1) occur. To ensure maximum sensitivity and linearity of the measured signals, the static path difference must be maintained at the optimum quadrature point. This is achieved when $\Delta d_{sc} = (2n-1)\lambda/8$. The photo detector output then becomes equation (2), and the absolute displacement of a very small ultrasonic oscillation d_{ac} may then be determined by simply multiplying the photo detector output by a known scale factor.

$$I = I_p + I_r + 2\sqrt{I_p I_r} \cdot (4\pi\ d_{ac}/\lambda) \tag{2}$$

Since low frequency but large amplitude phase fluctuations arising from environmental disturbances, such as room vibration and air turbulence, may cause the interferometer to drift out of quadrature, an active feedback controlled PZT actuator is employed to implement the needed path stabilization. It allows active control to shift the reference arm length to compensate any fluctuation caused by low frequency environmental disturbances, thus keeping the static path difference at the expected quadrature point. The control circuit is adjusted to minimize overshoot while maintaining a sufficient response speed. The control system can also generate a sinusoidal fluctuation to cause the reference mirror to vibrate with a displacement that is larger than the wavelength of the laser in order to get a full-scale response. The DC component of this response representing the desired stabilization position is used to set the reference value of the control circuit through a D/A plug-in board. The AC component of this response representing the actual sensitivity of the interferometer at this location allows us to do point-by-point auto calibration.

All the measurements are recorded by a digital oscilloscope and transferred to a computer via the GPIB interface for further data processing. A minimum resolvable surface displacement of 0.04nm (40pm) has been achieved when the interferometer is used on a polished test surface and is operated at a bandwidth of DC-20MHz, using time-average data processing. The experimental results show that the path-stabilized control is critical for very small displacement detection. The designed path stabilization loop control and the point-to-point auto calibration effectively eliminate the effects of variable quality of the surface of the sample being tested.

EXPERIMENTAL RESULTS AND DISCUSSION

Experimental Study of EMAT Generation of A Single Lamb Wave Mode

We only considered a frequency within the 1MHz~3MHz range that matches the bandwidth of our EMAT transducers. The specimens used in this investigation were steel and aluminum plates.

Three meander-line EMATs with three different spacings of the wires: δ_1=1.3mm denoted EMAT1, δ_2=0.86mm denoted EMAT2 and δ_3=1.00mm denoted EMAT3 were employed. The spacing sizes were selected to be half the wavelength of the desired s_0 or a_0 mode.

Figures 2a and 2b show the results when using EMAT1 and EMAT2, respectively, both as source and receiver, working in a pulse-echo mode. The received signals are the reflected waves from the edge of the plate.

Figures 2c~2e, 2f~2h and 2i~2j show the results of using EMAT1, EMAT2, EMAT3 respectively, only as transmitters and the path-stabilized interferometer as the detector. The received signals include the direct signals ($s_0(1)$ and $a_0(1)$) and the corresponding reflected signals from the edge of the plate ($s_0(2)$ and $a_0(2)$). The interferometer only picks up the normal component of each mode.

Figure 3 shows the experimental results together with theoretical dispersion curves of the lowest symmetrical (s_0) and antisymmetrical (a_0) modes for aluminum plates. It is the plot of the dimensionless wavelength/thickness ratio (λ/d) vs. f*d. Here we use dimensionless λ/d such that these dispersion curves are valid for variable thicknesses of plates. The actual operation points of the EMATs are also shown on the theoretical curves.

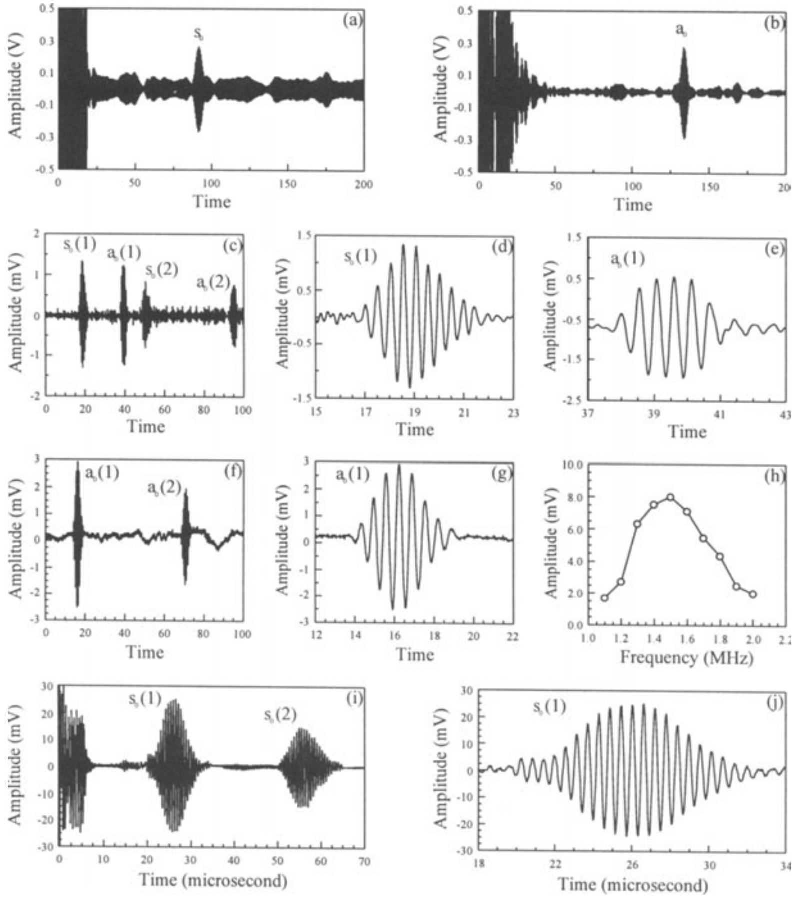

Figure 2. Experimental results for the analysis of the generated Lamb waves by EMATs. (a) EMAT1 both as source and receiver, (b) EMAT2 both as source and receiver, (c)~(e) EMAT1 as source and the laser interferometer as receiver, (f)~(h) EMAT2 as source and the laser interferometer as receiver, (i)~(j) EMAT3 as source and the laser interferometer as receiver.

The experimental results show the following:

- EMAT1, which was designed to generate the s_0 mode only, actually generated the s_0 mode (at 2MHz, C_g=4.9mm/μs) and the a_0 mode (at 1.9MHz, C_g=3.1mm/μs) simultaneously in a 0.75mm thick plate. It is worth noting that the a_0 mode was not picked up by EMAT detection (see Figure 2a).
- EMAT2, which was designed to generate the a_0 mode only, actually did generate only a single a_0 mode at any frequency within 1MHz to 2.5MHz in a 0.75mm thick plate. The amplitude of the generated a_0 is maximum when the center frequency is at 1.5MHz.
- EMAT3 generated only a single s_0 mode at 1.7MHz and only a single a_0 mode at 1.2MHz in a 1.5mm-thick aluminum plate. The same EMAT3 generated both s_0 and a_0 modes simultaneously at a frequency 1.5MHz.

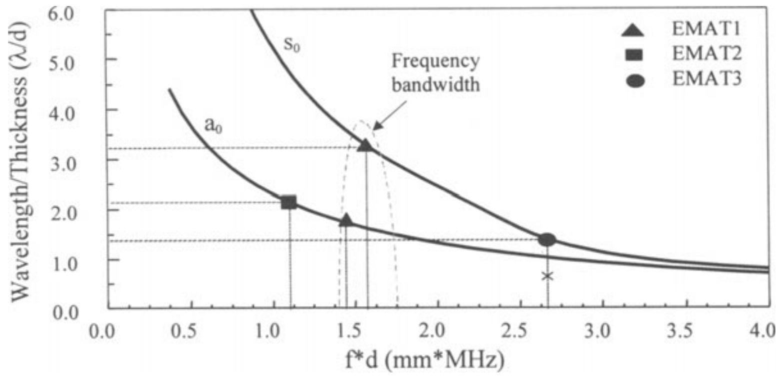

Figure 3. Plot of the theoretical dispersion curves of the lowest symmetrical (s_0) and antisymmetrical (a_0) modes and the actual operating points of EMAT1, EMAT2 and EMAT3, respectively.

From these results, we can draw the following conclusions. The spacing of the wires in the EMAT coil is critical to its behavior, the wave modes that EMATs can generate and pick up are dictated by this dimension with respect to plate thickness. By selecting the spacing size of the wires in the EMAT coil to be half the corresponding wavelength of the a_0 mode and keeping the frequency bandwidth small enough, we can generate a pure single a_0 mode, since the a_0 mode has the smallest wavelength compared with other modes at a given f*d. As for the generation of single s_0 mode, it is necessary to select an operation point at which the a_0 mode does not have a harmonic wavelength of the desired s_0 mode within the given f*d range. Otherwise, a harmonically related a_0 mode would also be excited. This is the reason why EMAT3 operating at 1.7MHz generated only the s_0 mode, but EMAT1 operating at 2MHz generated both s_0 and a_0 modes (shown in Figure 3). For the other higher modes, it may be more difficult, if not impossible, to avoid the harmonic lower modes coexisting, since they have higher wavelength.

Experimental Detection of Fatigue Cracks in A Riveted Aluminum Plate-Structure

As mentioned previously, Lamb waves probe the entire thickness and length of a plate and therefore interact with flaws anywhere in the structure along the probe path. It is therefore possible to find defects located either on the surface or internally using only single sided inspection. In this study, we investigated the scattered field resulting from the interaction of a single Lamb wave mode with a fatigue crack breaking from a rivet in a 1.5mm thick aluminum plate.

The experimental configuration is shown in Figure 4. We employed EMAT3 to generate a pure a_0 mode at 1.2MHz and a pure s_0 mode at 1.7MHz, respectively. The intention is to demonstrate the detection of cracks breaking from the rivet, and to compare the sensitivity of a_0 and s_0 modes for this type of defect, by means of EMAT generation and laser detection. Since this is a rough surface sample, we used the specially designed heterodyne interferometer developed in our center [11], to remotely monitor the scattered fields. The experimental procedure is as follows. Keep EMAT3's center aligned with the laser interferometer probe, and scan together with the laser probe to get B-scan

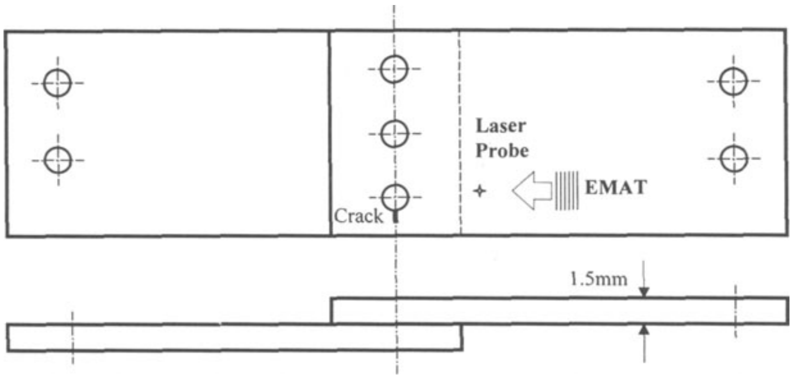

Figure 4. Configuration for experimental detection of fatigue cracks in a riveted thin plate-structure.

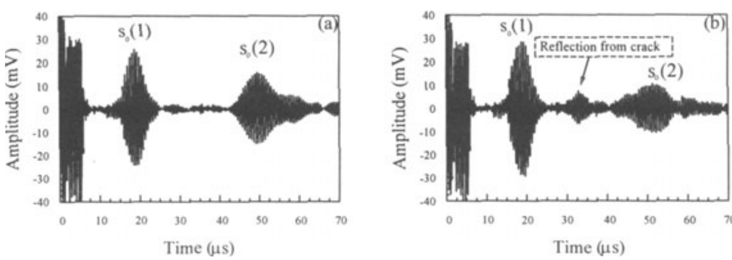

Figure 5. Detected waveforms corresponding to two special probing positions. (a) Crack is not inside the wave propagation path, (b) crack is inside the wave propagation path.

results ahead of the rivet. Figure 5 shows the detected waveforms corresponding to two special positions where a crack is outside and within the ultrasound path respectively.

CONCLUSIONS

In this paper, we described the configuration of a narrow-band EMAT ultrasound generation and a broadband path-stabilized Michelson interferometer detection system. This system was applied for the excitation of a single Lamb wave mode in a thin plate and for the investigation of fatigue cracks in riveted thin plates.

The experimental results show that the EMAT can be used as a well-defined narrow-band ultrasound source. In our study, a pure a_0 Lamb wave mode and a single s_0 mode have been generated respectively through careful design of the EMAT configuration and electrical resonance adjustments. The spacing of the wires in the EMAT is critical, as meander-line type EMATs tend to generate the wave mode whose wavelength is twice the spacing size. The experimental results are consistent with the theoretical predictions.

The laser interferometric detection used here provides the spatial resolution essential to monitor scattering from small flaws. The interferometric detection system employs an active path-stabilization feedback control and includes an automatic point-by-point calibration procedure to effectively eliminate the effects of variable surface quality of the sample under test.

By applying this EMAT generation of a single Lamb wave mode and the heterodyne interferometer detection, we experimentally explored the scattered fields resulting from the interaction of a single Lamb wave mode (s_0 or a_0) with a fatigue crack breaking from a rivet. Useful information concerning quantitative evaluation of these kinds of defects within thin plate structures has been extracted.

ACKNOWLEDGMENTS

This work was carried out in the course of research supported by the Office of Naval Research under Grant N00014-89-J-1362.

REFERENCES

1. Hirao, M., Ogi, H., and Fukuoka, H. "Resonance EMAT system for acoustoelastic stress measurement in sheet metals" *Review of Scientific Instruments* (1993) 64 (Nov.) 3198-3205
2. Gori, M., *et al.* "Guided-Waves by Emat Transducers for Rapid Defect Location on Heat-Exchanger and Boiler Tubes" *Ultrasonics* (1996) 34 (2-5) 311-314
3. Huang, J., Krishnaswamy, S., and Achenbach, J.D. "Laser generation of narrow-band surface waves" *J. Acoust. Soc. Am.* (1992) 92 (5) (11) 2527-2531
4. Nagata, Y., *et al.* "Lamb Wave Tomography Using Laser-Based Ultrasonics" *Review of Progress in Quantitative Nondestructive Evaluation* (1995) 14 561
5. Oursler, D.A. and Wagner, J.W. "Narrow-Band Hybrid Pulsed Laser/EMAT system for Noncontact Ultrasonic Inspection Using Angled Shear Waves" *Materials Evaluation* (1995) 53 (May) 593-597
6. Alleyne, D.N. and Cawley, P. "The Interaction of Lamb Waves with Defects" *IEEE Transactions on Ultrasonics,Ferroelectrics,and Frequency Control* (1992) 39 (No. 3) 381-396
7. Datta, S.K., Nassar, Y.A., and Shah, A.H. "Lamb Wave Scattering by a Surface-Breaking Crack in a Plate" *Review of Progress in Quantitative Nondestructive Evaluation* (1991) 10A 97-104
8. Guo, Z., Achenbach, J.D., and Krishnaswamy, S., "EMAT Generation and Laser Detection of Single Lamb Wave Modes" will be published in *Ultrasonics.*
9. Viktorov, I.A. *Rayleigh and Lamb Waves* Plenum Press, New York, 1967
10. Thompson, R.B. "Physical Principles of Measurements with EMAT Transducer" in *Physical Acoustics* edited by Thurston, R.N. and Piece, A.D. XIX Academic Press, Inc. San Diego (1990) 157-199
11. Pouet, B.F., et al. "Heterodyne interferometer with two-wave mixing in photorefractive crystals for ultrasound detection on rough surfaces" *Appl. Phys. Lett.* (1996) 69 (25) 16 December 3782-3784